Heavy Quark Diffusion from 2 + 1 Flavor Lattice QCD with 320 MeV Pion Mass

Luis Altenkort[1,*], Olaf Kaczmarek,[1] Rasmus Larsen,[2] Swagato Mukherjee,[3]
Peter Petreczky,[3] Hai-Tao Shu,[4,†] and Simon Stendebach[5]

(HotQCD Collaboration)

[1]*Fakultät für Physik, Universität Bielefeld, D-33615 Bielefeld, Germany*
[2]*Department of Mathematics and Physics, University of Stavanger, Stavanger, Norway*
[3]*Physics Department, Brookhaven National Laboratory, Upton, New York 11973, USA*
[4]*Institut für Theoretische Physik, Universität Regensburg, D-93040 Regensburg, Germany*
[5]*Insitut für Kernphysik, Technische Universität Darmstadt, Schlossgartenstraße 2, D-64289 Darmstadt, Germany*

We present the first calculations of the heavy flavor diffusion coefficient using lattice QCD with light dynamical quarks corresponding to a pion mass of around 320 MeV. For temperatures 195 MeV $< T <$ 352 MeV, the heavy quark spatial diffusion coefficient is found to be significantly smaller than previous quenched lattice QCD and recent phenomenological estimates. The result implies very fast hydrodynamization of heavy quarks in the quark-gluon plasma created during ultrarelativistic heavy-ion collision experiments.

Introduction.—Heavy charm and bottom quarks are produced only during the earliest stages of ultrarelativistic heavy-ion collisions. They participate in the entire evolution of the quark-gluon plasma (QGP), and emerge as open heavy-flavor hadrons or quarkonia. These heavy-flavor hadrons provide valuable insights into the QGP. Experiments at the relativistic heavy ion collider (RHIC) and large hadron collider (LHC) show that the yields of heavy flavor hadrons at low transverse momentum (p_T) are asymmetric along the azimuthal angle, meaning that the elliptic flow parameter (v_2) is large [1–3]. These observations indicate that heavy quarks participate in the hydrodynamic expansion of the QGP. Understanding the origin of the hydrodynamic behavior of heavy quarks is key to understanding the near-perfect fluidity of the QGP.

The motion of a heavy quark with mass $M \gg T$, immersed in a QGP at temperature T, can be effectively described by Langevin dynamics [4]. The heavy quark momentum diffusion coefficient, κ, quantifies the momentum transfer to the heavy quark from the QGP background through random momentum kicks which are uncorrelated in time. Specifically, 3κ is the mean squared momentum transfer per unit time. For sufficiently low p_T,

hydrodynamization of heavy quarks in the QGP can be characterized by the diffusion constant in space $D_s = 2T^2/\kappa$ [4], where $6D_s$ is the mean squared distance traversed per unit time by the heavy quark inside the QGP. The available perturbative QCD results for κ [5] provide reliable estimates only for asymptotically large T. For practical phenomenological studies of heavy-ion collisions lattice QCD results for κ are needed. Until now, lattice QCD based determinations of κ have been limited only to pure gauge theory, therefore neglecting dynamical fermions entirely. Here, we report the first continuum-extrapolated lattice QCD calculations of κ in $2 + 1$-flavor QCD with a physical strange quark mass and degenerate up and down quark masses corresponding to a pion mass $m_\pi \simeq 320$ MeV.

Theoretical framework.—The momentum diffusion coefficient κ can be obtained from the zero-frequency limit of the spectral function corresponding to the conserved current-current correlation function of heavy quarks. Relying on $M \gg T$ and $M \gg \Lambda_{\text{QCD}}$, the QCD Lagrangian can be expanded in powers of $1/M$. By integrating out the heavy quark fields one arrives at the heavy quark effective theory. In this effective theory the heavy-quark current-current correlator at leading order in $1/M$ becomes equivalent to the correlation function of the color-electric field [6,7]:

$$G_E = -\sum_{i=1}^{3} \frac{\langle \text{ReTr}[U(1/T, \tau) E_i(\tau, \mathbf{0}) U(\tau, 0) E_i(0, \mathbf{0})] \rangle}{3 \langle \text{ReTr} U(1/T, 0) \rangle}.$$

(1)

Here, $U(\tau_1, \tau_2)$ is the temporal Wilson line between Euclidean time τ_1 and τ_2, and $E_i(\mathbf{x}, \tau) = U_i(\mathbf{x}, \tau)U_4(\mathbf{x} + \hat{i}, \tau) - U_4(\mathbf{x}, \tau)U_i(\mathbf{x} + \hat{4})$ is the discretized chromoelectric field [7]. G_E receives only a finite renormalization at nonzero lattice spacing [8]. In the continuum limit the corresponding spectral function, $\rho_E(\omega, T)$, can be obtained by inverting [7]:

$$G_E(\tau, T) = \int_0^\infty \frac{d\omega}{\pi} \rho_E(\omega, T) \frac{\cosh[\omega\tau - \omega/(2T))]}{\sinh[\omega/(2T)]}, \quad (2)$$

where

$$\kappa(T) = 2T \lim_{\omega \to 0} [\rho_E(\omega, T)/\omega], \quad (3)$$

up to corrections proportional to T/M.

The leading order (LO) [7] and next-to-leading order (NLO) [7] perturbative QCD estimates predict $\rho_E(\omega, T) \propto \omega^3$, which should be valid for sufficiently large T and/or ω. Therefore, $G_E(\tau, T)$ is expected to receive significant contributions also from the high-frequency regions.

Lattice QCD calculations.—We performed calculations in $2 + 1$ flavor QCD with a physical strange quark mass, m_s, and degenerate up, down quark masses $m_l = m_s/5$ using the highly improved staggered quark (HISQ) action [9] and tree-level improved Lüscher-Weisz gauge action [10,11]. In the continuum limit our choice of m_l corresponds to $m_\pi \simeq 320$ MeV. The lattice spacing a and the quark masses are fixed as in Refs. [12,13]. We carried out calculations on $96^3 \times N_\tau$ lattices with $1/a = 7.036$ GeV and $N_\tau = 20$, 24, 28, 32, and 36, that correspond to temperatures $T = 352$, 293, 251, 220, and 195 MeV, respectively. To control discretization effects we also performed calculations on $64^3 \times N_\tau$ lattices ($N_\tau = 20$, 22, and 24) at different lattice spacings, chosen such that the above temperature values are reproduced. Further details on the lattice setup are given in the Supplemental Material [14].

Naive measurements of $G_E(\tau, T)$ are highly susceptible to high-frequency fluctuations in the gauge fields and exhibit a poor signal-to-noise ratio. In quenched QCD, the multilevel algorithm [43] has been applied to overcome this problem. However, this algorithm is not applicable for QCD with dynamical fermions. To overcome the noise problem for our calculations with dynamical fermions we use the Symanzik-improved [15] gradient flow [44]. In quenched QCD it was demonstrated [16,17] that this approach is as effective as the multi-level algorithm for noise reduction, while also renormalizing G_E nonperturbatively. By evolving the gauge fields in the fictitious flow time, τ_F, as dictated by the force given by the gradient of the gauge action, the gradient flow smears the gauge fields over the radius $\sqrt{8\tau_F}$. Renormalization artifacts of the electric field operators E_i due to finite lattice spacing a are highly

suppressed for $\sqrt{8\tau_F} > a$. However, the flow radius should always be smaller than the relevant physical scales, implying the constraint $\sqrt{8\tau_F} < \tau < 1/(2T)$.

For G_E it was found that the more strict criterion $\sqrt{8\tau_F}/\tau < 1/3$ should be respected [16,17,45].

Results.—Since $\rho_E \propto \omega^3$ for large ω, G_E is a steeply falling function of τ. Therefore, it is convenient to normalize it by the leading-order perturbative result [7], with the Casimir factor, $C_F = 4/3$, and the coupling constant, g, scaled out, that is, with $G^{\text{norm}} \equiv G_E^{\text{LO}}/(g^2 C_F)$.

At small τ the lattice results will suffer from significant discretization effects. Furthermore, the distortions of the correlation functions due to gradient flow are the largest at small τ. The cutoff effects as well as the distortions due to gradient flow are also present in the free field theory. We can use the free theory result to estimate and partly correct for these effects. To reduce lattice cutoff effects as well as distortions due to gradient flow we perform tree-level improvement, meaning that we multiply the chromoelectric correlator by the ratio of the free correlator obtained in the continuum and the one calculated on the lattice (in perturbation theory) with the given N_τ at nonzero flow time: $G_E(\tau, T) \to G_E(\tau, T) \times [G^{\text{norm}}(\tau T)/G_{\tau_F}^{\text{norm}}(\tau T, N_\tau)]$. The details of calculating $G_{\tau_F}^{\text{norm}}(\tau T, N_\tau)$ can be found in Supplemental Material [14].

The lattice chromo-electric correlators after tree-level improvement and normalized by G^{norm} for the $96^3 \times N_\tau$ lattices are shown in Fig. 1. We show the results for two different amounts of gradient flow, adjusted for each separation τ by fixing $\sqrt{8\tau_F}/\tau$. In addition, we show the results from the coarsest lattices (64^3) as open symbols. We see that gradient flow is effective in reducing UV noise even for the largest lattice with $N_\tau = 36$. After tree-level improvement, the difference of G_E/G^{norm} obtained on the finest and the coarsest lattice is generally smaller than the statistical errors of the data obtained on the finest lattice. The flow time dependence is also quite small for $\tau T > 0.25$ if the ratio of the flow radius $\sqrt{8\tau_F}$ to τ is between 0.25 and 0.3. For $\tau T < 0.25$ the amount of flow necessary to suppress discretization artifacts already comes close to the relevant physical scale of $\tau/3$, leading to large distortions. For this reason the corresponding data points need to be omitted from the analysis.

Naively one expects that at high (but not extremely high) temperatures G_E/G^{norm} should not be different from unity since $G_E^{\text{LO}} \approx g^2 C_F$ is a good approximation for G_E and $C_F g^2 \simeq 1$. An interesting feature of the results shown in Fig. 1 is that the ratio G_E/G^{norm} has a much larger deviation from one than in the quenched case. In quenched QCD, G_E/G^{norm} reaches a value of about 4 at most [18]. This is due to the fact that the τ values in physical units (fm) accessible in full QCD are larger and, as we will see later, the value of κ in temperature units also turn out to be larger. As in quenched QCD, deviations from unity of G_E/G^{norm}
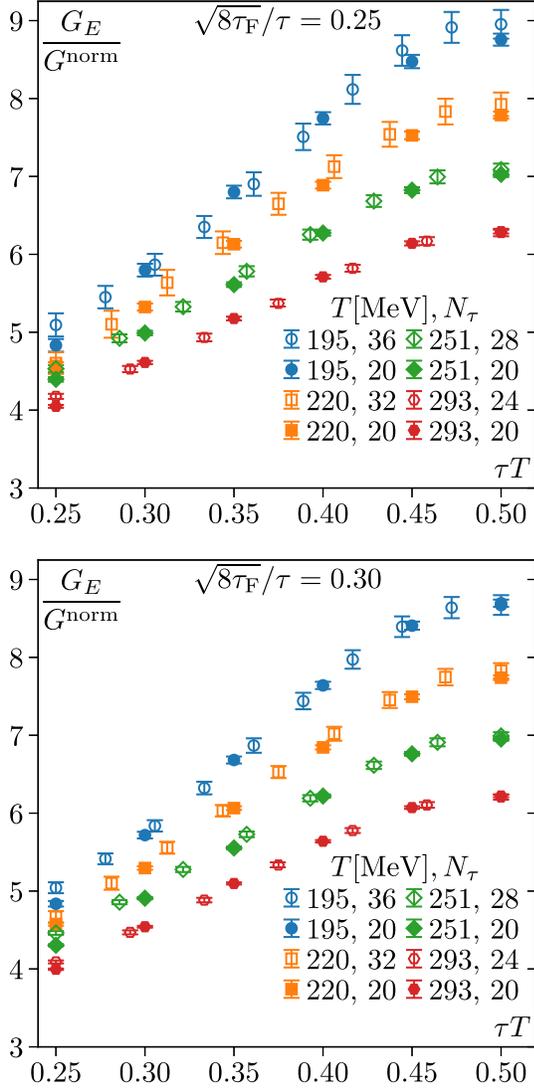
FIG. 1.   The chromoelectric correlator normalized by its weak-coupling structure at tree level (G^{norm}) as a function of τ calculated on the $96^3 \times N_\tau$ lattices (open symbols) and $64^3 \times 20$ lattices (filled symbols) at two different flow times in units of τ.

FIG. 2.   The continuum and zero flow time extrapolated results for the chromoelectric correlator at different temperatures as a function of τT. Also shown is the result for the highest temperature at nonzero lattice spacing corresponding to $N_\tau = 20$ and flow time $\sqrt{8\tau_{\mathrm{F}}}/\tau = 0.3$. The dashed lines indicate fitted model correlators for the "smax" model using the NLO ρ_{UV}.

are the largest at the lowest temperature, and become smaller as the temperature increases.

Next, we perform the continuum and flow-time-to-zero extrapolation of the chromoelectric correlator. First, we interpolate the correlators obtained on $64^3 \times N_\tau$ lattices in τ for various values of τ_{F}/τ^2. From these interpolations we determine the correlator on coarser lattices for values of τ that are available for the finest $96^3 \times N_\tau$ lattices and then perform continuum extrapolations for each τT and τ_{F}/τ^2. As is apparent from Fig. 1, the cutoff effects are small except for small values of τT. We perform the continuum extrapolation assuming that discretization errors go like $(aT)^2 \sim 1/N_\tau^2$, which turns out to be capable of describing our data well; see Supplemental Material [14].

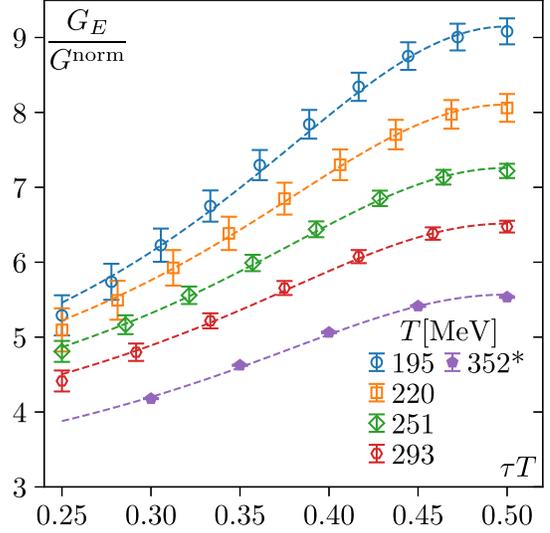Finally, we perform the flow-time-to-zero extrapolation of the chromoelectric correlators. In the region $a \ll \sqrt{8\tau_{\mathrm{F}}} \ll \tau$ we expect a linear τ_{F} dependence as suggested by NLO perturbation theory [19]. And indeed, for $0.25 < \sqrt{8\tau_{\mathrm{F}}}/\tau < 0.3$ a linear dependence seems to describe the data. Therefore, we use a linear extrapolation in τ_F in this region to obtain the zero flow time limit, see Supplemental Material [14]. The continuum and zero flow time extrapolated results for the chromoelectric correlators are shown in Fig. 2. The extrapolations do not change the qualitative features of the correlation function but lead to a significant increase of the statistical errors.

With the continuum and flow-time-extrapolated data for the chromoelectric correlator we are in the position to estimate the heavy quark diffusion coefficient κ. To do so we need a parametrization of the spectral function that enters Eq. (2). Any parametrization of the spectral function should take into account its known behavior at small and large ω. For small ω the spectral function is solely determined by the heavy quark diffusion coefficient and has the form [7]: $\rho_E(\omega, T) \simeq \rho_{\mathrm{IR}}(\omega, T) = \kappa \omega/(2T)$ while at sufficiently large frequency the ω dependence of the spectral function should be described by perturbation theory due to asymptotic freedom in QCD. Moreover, thermal corrections to the spectral function are very small for $\omega \gg T$. Therefore, we assume that at large energies the spectral function is given by the LO or NLO perturbative $T = 0$ result up to a constant: $\rho_E(\omega \gg T) = \rho_{\mathrm{UV}}(\omega) = K\rho_{\mathrm{LO,NLO}}(\omega)$. The factor K accounts for the fact that the perturbative calculations may not be quantitatively reliable due to missing contributions from higher orders.

Perturbative calculations at NLO [7,20], classical simulations in effective three-dimensional theory [21], and

strong coupling calculations [22] show that the spectral function is a smooth monotonically rising function of ω. Based on this, as well as the above considerations, we use the following two forms of the spectral function in our analysis that also have been used already in quenched QCD [18,23]: $\rho_{\max} = \max(\rho_{\mathrm{IR}}(\omega, T), \rho_{\mathrm{UV}}(\omega))$ and $\rho_{\mathrm{smax}} = \sqrt{\rho_{\mathrm{IR}}^2(\omega, T) + \rho_{\mathrm{UV}}^2(\omega)}$, which we refer to as the maximum (max) and the smooth maximum (smax) *Ansätze*, respectively. The latter is consistent with the perturbative NLO calculation [20] and OPE considerations [46] when it comes to the leading thermal correction at $\omega \gg T$. We also consider a third *Ansatz* for the spectral function, that is given by $\rho_{\mathrm{IR}}(\omega, T)$ up to $\omega = \omega_{\mathrm{IR}}$, and by ρ_{UV} for $\omega > \omega_{\mathrm{UV}}$, and for $\omega_{\mathrm{IR}} < \omega < \omega_{\mathrm{UV}}$ we interpolate with a power-law form $\rho(\omega, T) = c\omega^p$. The parameters c and p are chosen such that the spectral function is continuous at $\omega = \omega_{\mathrm{IR}}$ and ω_{UV}. This form of the spectral function has been used in Ref. [18]. Based on theoretical results we choose $\omega_{\mathrm{IR}} = T$ and $\omega_{\mathrm{UV}} = 2\pi T$, see Supplemental Material [14].

Using the above three *Ansätze* for the spectral functions and the spectral representation of the chromoelectric correlator we fitted the continuum- and flow-time-extrapolated results treating κ and K as fit parameters and thus estimated the heavy quark diffusion coefficient. It turns out that the maximum *Ansatz* gives the largest value of κ, while the power-law form gives the smallest value. Using the LO or NLO form of ρ_{UV} does not lead to significant change in the value of κ, meaning that the estimated values of κ are not too sensitive to the modeling of the high energy part of the spectral function.

Each model is fitted onto the same 1000 bootstrap samples of the double-extrapolated correlator data. We collect all results from all models in a single "distribution" for the fit parameter κ/T^3. We determine a confidence interval by considering the median of this distribution, and then adding or subtracting the 34th percentiles on each side, which gives the lower and upper bounds of the interval. For better readability we quote the central value of the interval with the distance to the bounds as the uncertainty. We obtain $\kappa(T=195\,\mathrm{MeV})=11.0(2.5)T^3$, $\kappa(T=220\,\mathrm{MeV})=8.4(2.4)T^3$, $\kappa(T = 251\,\mathrm{MeV}) = 6.9(2.2)T^3$, and $\kappa(T = 293\,\mathrm{MeV}) = 5.8(2.0)T^3$.

As already noted above, the shape of the correlation function for $\tau T > 0.25$ does not seem to be significantly changed by the continuum and flow-time-to-zero extrapolations. Therefore, we also performed the above analysis using the nonzero lattice spacing data at $1/a = 7.036$ GeV and nonzero relative flow times $\sqrt{8\tau_F}/\tau = 0.3$. We find that the estimated values of κ agree with the ones obtained from the continuum- and flow-time-extrapolated data within errors. This is due to the fact that the systematic uncertainties associated with modeling of the spectral function are much larger than the effect of the continuum and zero-flow-time extrapolation. For this reason we also
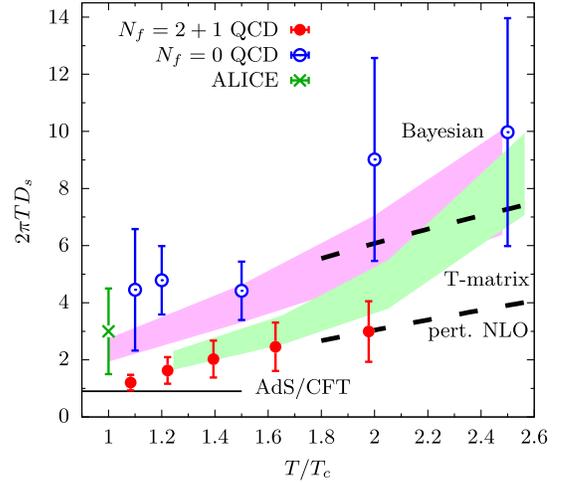

FIG. 3. The spatial heavy quark diffusion coefficient in units of $2\pi T$ from our lattice calculations compared to the AdS/CFT estimate [6], NLO perturbative calculation [5], and the quenched lattice QCD calculations [16,18,24]. For the quenched lattice data we show the result of Ref. [18] for $T = 1.1T_c$, the result of Ref. [16] for $T = 1.5T_c$, and the results of Ref. [24] for the remaining temperatures. For the NLO calculations we used two values of the renormalization scale, $\mu = 2\pi T$ (lower dashed line) and $\mu = 4\pi T$ (upper dashed line). Also shown are the phenomenological estimates [48–51], see main text.

estimate the heavy quark diffusion coefficient at nonzero lattice spacing and flow time for the highest temperature resulting in $\kappa(T = 356\,\mathrm{MeV})/T^3 = 4.8(1.7)$.

Conclusion.—We carried out first lattice QCD calculations of the heavy quark diffusion constant in $2 + 1$ flavor QCD at leading order in the inverse heavy quark mass and in the phenomenologically relevant region of 195 MeV $< T <$ 352 MeV. Our results for D_s as function of T/T_c are summarized in Fig. 3. Here we use $T_c = 180$ MeV because the calculations are performed at $m_\pi \simeq 320$ MeV, see Supplemental Material [14]. Our results are smaller than the quenched lattice QCD results [18,24]. At the lowest temperature our result agrees, within errors, with the strong coupling expectations from AdS/CFT [6,47]. At the highest temperature our result D_s is compatible with the NLO perturbative prediction [5] within the uncertainties. In comparisons to some phenomenological determinations, namely, the Bayesian analysis [48] of heavy-ion collision data, and the ALICE Collaboration's model fits to their data [49], the lattice QCD results for D_s are systematically smaller. On the other hand, the T-matrix approach on D_s [50,51] seems to agree with the lattice results.

The present study can be extended in two different ways. Based on the previous lattice QCD studies of QCD equation of state [13], quark number susceptibilities [25,52], and static quark free energies [53] with light quark mass $m_l = m_s/5$ compared to those with nearly physical light quark mass $m_l \simeq m_s/20$, we expect the effect larger

than physical quark mass on D_s to be small in the temperature range considered in this study. However, such effects might be significant for temperatures closer to the QCD crossover temperature. Thus, we plan to extend the present calculations to smaller temperatures with physical values of the light quark masses. The heavy quark mass suppressed effects to the heavy quark diffusion coefficients are expected to be relatively small based on the calculations performed in quenched QCD [17,54]. We plan to estimate these corrections also in $2 + 1$ flavor QCD.

*altenkort@physik.uni-bielefeld.de
†hai-tao.shu@ur.de

[1] A. Beraudo *et al.*, Nucl. Phys. **A979**, 21 (2018).
[2] X. Dong, Y.-J. Lee, and R. Rapp, Annu. Rev. Nucl. Part. Sci. **69**, 417 (2019).
[3] M. He, H. van Hees, and R. Rapp, Prog. Part. Nucl. Phys. **130**, 104020 (2023).
[4] G. D. Moore and D. Teaney, Phys. Rev. C **71**, 064904 (2005).
[5] S. Caron-Huot and G. D. Moore, Phys. Rev. Lett. **100**, 052301 (2008).
[6] J. Casalderrey-Solana and D. Teaney, Phys. Rev. D **74**, 085012 (2006).
[7] S. Caron-Huot, M. Laine, and G. D. Moore, J. High Energy Phys. 04 (2009) 053.
[8] C. Christensen and M. Laine, Phys. Lett. B **755**, 316 (2016).
[9] E. Follana, Q. Mason, C. Davies, K. Hornbostel, G. P. Lepage, J. Shigemitsu, H. Trottier, and K. Wong (HPQCD/ UKQCD Collaboration), Phys. Rev. D **75**, 054502 (2007).
[10] M. Luscher and P. Weisz, Commun. Math. Phys. **97**, 59 (1985); **98**, 433(E) (1985).
[11] M. Luscher and P. Weisz, Phys. Lett. B **158**, 250 (1985).
[12] A. Bazavov *et al.* (HotQCD Collaboration), Phys. Rev. D **90**, 094503 (2014).
[13] A. Bazavov, P. Petreczky, and J. H. Weber, Phys. Rev. D **97**, 014510 (2018).
[14] See Supplemental Material at http://link.aps.org/ supplemental/10.1103/PhysRevLett.130.231902 for the technical details of this study, which includes Refs. [7,12,13,15–42].
[15] A. Ramos and S. Sint, Eur. Phys. J. C **76**, 15 (2016).
[16] L. Altenkort, A. M. Eller, O. Kaczmarek, L. Mazur, G. D. Moore, and H.-T. Shu, Phys. Rev. D **103**, 014511 (2021).
[17] N. Brambilla, V. Leino, J. Mayer-Steudte, and P. Petreczky (TUMQCD Collaboration), Phys. Rev. D **107**, 054508 (2023).
[18] N. Brambilla, V. Leino, P. Petreczky, and A. Vairo, Phys. Rev. D **102**, 074503 (2020).
[19] A. M. Eller, The color-electric field correlator under gradient flow at next-to-leading order in quantum chromodynamics, Ph.D. thesis, Technische Universität, Dortmund (main), Darmstadt, Tech. Hochsch., 2021.
[20] Y. Burnier, M. Laine, J. Langelage, and L. Mether, J. High Energy Phys. 08 (2010) 094.
[21] M. Laine, G. D. Moore, O. Philipsen, and M. Tassler, J. High Energy Phys. 05 (2009) 014.
[22] S. S. Gubser, Nucl. Phys. **B790**, 175 (2008).
[23] A. Francis, O. Kaczmarek, M. Laine, T. Neuhaus, and H. Ohno, Phys. Rev. D **92**, 116003 (2015).
[24] D. Banerjee, R. Gavai, S. Datta, and P. Majumdar, arXiv:2206.15471.
[25] A. Bazavov and P. Petreczky (HotQCD Collaboration), J. Phys. Conf. Ser. **230**, 012014 (2010).
[26] S. Stendebach, Perturbative analysis of operators under improved gradient flow in lattice QCD, Master's thesis, Technische Universität Darmstadt, 2022.
[27] K. Kajantie, M. Laine, K. Rummukainen, and M. E. Shaposhnikov, Nucl. Phys. **B503**, 357 (1997).
[28] F. Herren and M. Steinhauser, Comput. Phys. Commun. **224**, 333 (2018).
[29] K. G. Chetyrkin, J. H. Kuhn, and M. Steinhauser, Comput. Phys. Commun. **133**, 43 (2000).
[30] Y. Aoki *et al.* (Flavour Lattice Averaging Group (FLAG) Collaboration), Eur. Phys. J. C **82**, 869 (2022).

[31] C. McNeile, C. T. H. Davies, E. Follana, K. Hornbostel, and G. P. Lepage, Phys. Rev. D **82,** 034512 (2010).

[32] B. Chakraborty, C. T. H. Davies, B. Galloway, P. Knecht, J. Koponen, G. C. Donald, R. J. Dowdall, G. P. Lepage, and C. McNeile, Phys. Rev. D **91,** 054508 (2015).

[33] C. Ayala, X. Lobregat, and A. Pineda, J. High Energy Phys. 09 (2020) 016.

[34] A. Bazavov, N. Brambilla, X. Garcia i Tormo, P. Petreczky, J. Soto, A. Vairo, and J. H. Weber (TUMQCD Collaboration), Phys. Rev. D **100,** 114511 (2019).

[35] S. Cali, K. Cichy, P. Korcyl, and J. Simeth, Phys. Rev. Lett. **125,** 242002 (2020).

[36] M. Bruno, M. Dalla Brida, P. Fritzsch, T. Korzec, A. Ramos, S. Schaefer, H. Simma, S. Sint, and R. Sommer (ALPHA Collaboration), Phys. Rev. Lett. **119,** 102001 (2017).

[37] S. Aoki *et al.* (PACS-CS Collaboration), J. High Energy Phys. 10 (2009) 053.

[38] K. Maltman, D. Leinweber, P. Moran, and A. Sternbeck, Phys. Rev. D **78,** 114504 (2008).

[39] D. Banerjee, S. Datta, R. Gavai, and P. Majumdar, Phys. Rev. D **85,** 014510 (2012).

[40] F. Karsch, E. Laermann, P. Petreczky, and S. Stickan, Phys. Rev. D **68,** 014504 (2003).

[41] S. Stickan, F. Karsch, E. Laermann, and P. Petreczky, Nucl. Phys. B, Proc. Suppl. **129,** 599 (2004).

[42] A. Bazavov *et al.* (MILC Collaboration), Proc. Sci., LATTICE2010 (**2010**) 074.

[43] M. Luscher and P. Weisz, J. High Energy Phys. 09 (2001) 010.

[44] M. Lüscher, J. High Energy Phys. 08 (2010) 071; 03 (2014) 92.

[45] A. M. Eller and G. D. Moore, Phys. Rev. D **97,** 114507 (2018).

[46] S. Caron-Huot, Phys. Rev. D **79,** 125009 (2009).

[47] O. Andreev, Mod. Phys. Lett. A **33,** 1850041 (2018).

[48] Y. Xu, J. E. Bernhard, S. A. Bass, M. Nahrgang, and S. Cao, Phys. Rev. C **97,** 014907 (2018).

[49] S. Acharya *et al.* (ALICE Collaboration), J. High Energy Phys. 01 (2022) 174.

[50] S. Y. F. Liu and R. Rapp, Eur. Phys. J. A **56,** 44 (2020).

[51] S. Y. F. Liu and R. Rapp, Phys. Rev. C **97,** 034918 (2018).

[52] A. Bazavov and P. Petreczky (HotQCD Collaboration), Phys. Part. Nucl. Lett. **8,** 860 (2011).

[53] A. Bazavov, N. Brambilla, P. Petreczky, A. Vairo, and J. H. Weber (TUMQCD Collaboration), Phys. Rev. D **98,** 054511 (2018).

[54] D. Banerjee, S. Datta, and M. Laine, J. High Energy Phys. 08 (2022) 128.

[55] L. Mazur, Topological aspects in lattice QCD, Ph.D. thesis, Bielefeld University, 2021, 10.4119/unibi/2956493.

[56] D. Bollweg, L. Altenkort, D. A. Clarke, O. Kaczmarek, L. Mazur, C. Schmidt, P. Scior, and H.-T. Shu, Proc. Sci., LATTICE2021 (**2022**) 196 [arXiv:2111.10354].

[57] L. Altenkort, O. Kaczmarek, R. Larsen, S. Mukherjee, P. Petreczky, H.-T. Shu, and S. Stendebach, Data publication: Heavy Quark Diffusion from $2+1$ Flavor Lattice QCD, Bielefeld University, 2023, 10.4119/unibi/2979080.